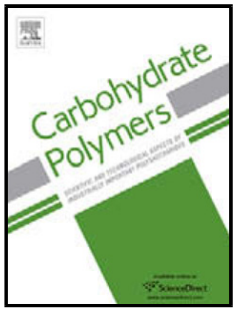

Title: Single molecule investigation of the onset and minimum size of the Calcium-mediated junction zone in alginate

Author: Kate A. Bowman Olav Andreas Aarstad Marcela Nakamura Bjørn Torger Stokke Gudmund Skjåk-Bræk Andrew N. Round

PII: S0144-8617(16)30404-0
DOI: http://dx.doi.org/doi:10.1016/j.carbpol.2016.04.043
Reference: CARP 10983

To appear in:

Received date: 25-2-2016
Revised date: 8-4-2016
Accepted date: 9-4-2016

Please cite this article as: Bowman, Kate A., Aarstad, Olav Andreas., Nakamura, Marcela., Stokke, Bjorn Torger., Skjåk-Braek, Gudmund., & Round, Andrew N., Single molecule investigation of the onset and minimum size of the Calcium-mediated junction zone in alginate.*Carbohydrate Polymers* http://dx.doi.org/10.1016/j.carbpol.2016.04.043

Single molecule investigation of the onset and minimum size of the Calcium-mediated junction zone in alginate

Kate A. Bowman[1], Olav Andreas Aarstad[2], Marcela Nakamura[1,3], Bjørn Torger Stokke[4], Gudmund Skjåk-Bræk[2] and Andrew N. Round[1]

1 University of East Anglia, School of Pharmacy (United Kingdom); **2** Norwegian University of Science and Technology, Department of Biotechnology (Norway); **3** University of São Paulo, Ribeirão Preto School of Pharmaceutical Sciences; **4** Norwegian University of Science and Technology, Department of Physics

*Corresponding author.

Highlights

- Ca^{2+}-mediated crosslinking of oligoguluronic acids ("oligoGs") with dp 6-20 was studied by single molecule force spectroscopy.
- The minimum length of an oligoG required to form a stable eggbox junction zone is 8 monomers.
- The work required to separate a pair of oligoGs after short (< 20 ms) interaction times is highest for the shortest stable eggbox junctions.
- At longer interaction times (up to 500 ms) the crosslinks formed between the longest dp oligoGs require the greatest work to separate.
- The rapid formation of Ca^{2+}-mediated interactions between single guluronic acids outcompetes, and subsequently constrains, the formation of stable eggbox junctions.
- This competition between crosslinking modes accounts for the long relaxation times seen during the formation of alginate gels.

Abstract

One of the principal roles of alginate, both natively and in commercial applications, is gelation via Ca^{2+}-mediated crosslinks between blocks of guluronic acid. In this work, single molecule measurements were carried out between well-characterised series of nearly monodisperse guluronic acid blocks ('oligoGs') using dynamic force spectroscopy. The measurements provide evidence that for interaction times on the order of tens of milliseconds the maximum crosslink strength is achieved by pairs of oligoGs long enough to allow the coordination of 4 Ca^{2+} ions, with both shorter and longer oligomers forming weaker links. Extending the interaction time from tens to hundreds of milliseconds allows longer oligoGs to achieve much stronger crosslinks but does not change the strength of individual links between shorter oligoGs. These results are considered in light of extant models for the onset of cooperative crosslinking in polyelectrolytes and an anisotropic distribution of oligoGs on interacting surfaces and provide a timescale for the formation and relaxation of alginate gels at the single crosslink level.

Keywords: alginate; gel; junction zone; single molecule; AFM

1. Introduction

Alginate is the collective term for a group of binary copolymeric polysaccharides synthesised by some algae and bacteria (Draget, Smidsrød, & Skjåk-Bræk, 2005; Gorin & Spencer, 1966; Linker & Jones, 1966). The two monomers comprising the copolymer are α-L-guluronic acid ('G') and β-D-mannuronic acid ('M'). Since M and G are epimers of each other, the alginate polymer is synthesised as polymannuronic acid and epimerisation of individual residues within the polymannuronic acid chain to guluronic acids is carried out by a family of epimerases (Haug & Larsen, 1971a, b; Larsen & Haug 1971). This enzymatic epimerisation results in varied patterns of the sequences GMG and GG being generated within the polymannuronic acid, with different

organisms having different epimerases that make alginates specific to each species (Campa et al., 2004; Hartmann, Holm, Johansen, Skjåk-Bræk, & Stokke, 2002; Høidal, Ertesvåg, Skjåk-Bræk, Stokke, & Valla, 1999; Holtan, Zhang, Strand, & Skjåk-Bræk, 2006).

The key function of alginates, both in vivo and as exploited commercially, is their gelling ability (Draget, Skjåk-Bræk, & Smidsrød, 1997; Draget & Taylor, 2011). The chief mechanism of gelation in alginates is through the metal cation (typically Ca^{2+})-mediated formation of so-called 'eggbox' junction zone crosslinks between sequences of Gs in interacting polymers of alginate (Grant, Morris, Rees, Smith, & Thom, 1973): multiple pairs of neighbouring G residues on opposing alginate chains are coordinated by Ca^{2+} ions that fit into the pockets created by the G pairs, resembling eggs in an eggbox (see **Figure 1** for an illustration). More recent evidence for the eggbox junction zone configuration comes from detailed X-ray diffraction studies (Sikorski, Mo, Skjåk-Bræk, & Stokke, 2007), and its importance as a gelling mechanism is borne out by the finding that alginates comprising long uninterrupted sequences of polyG form the strongest gels in the presence of divalent cations (Skjåk-Bræk, Smidsrød, & Larsen, 1986). More recently still, molecular dynamic and Monte Carlo simulations (Plazinski, 2011; Stewart, Grey, Vasiljevic, & Orbell, 2014) have revealed alternative Ca^{2+}-dependent modes of crosslinking two or more polyG strands, including variants of the eggbox junction as well as a perpendicular junction involving two polyG strands and three Ca^{2+} ions, while a similar ‘tilted eggbox’ crosslink has been proposed independently (Borgogna, Skjåk-Bræk, Paoletti, & Donati, 2013) to reflect the intial stages of crosslinking between two alginate strands. The minimum length of an oligoguluronate (oligoG) necessary to form a strong eggbox junction zone has been considered to be eight residues (allowing for four Ca^{2+} ions to be crosslinked) based upon a cooperative model for junction formation (Stokke, Smidsrød, Bruheim, & Skjåk-Bræk, 1991) and corroborated by leaching studies that showed only polymers with polyG sequences shorter than eight were leached from Ca-alginate gels (Stokke, Smidsrød, Zanetti, Strand, & Skjåk-Bræk, 1993). A detailed analysis of the dependence of

the strength of the Ca^{2+}-mediated interaction between oligoGs on the length of oligoG sequences, however, has not been carried out before, due in part to the lack of well-characterised oligoGs.

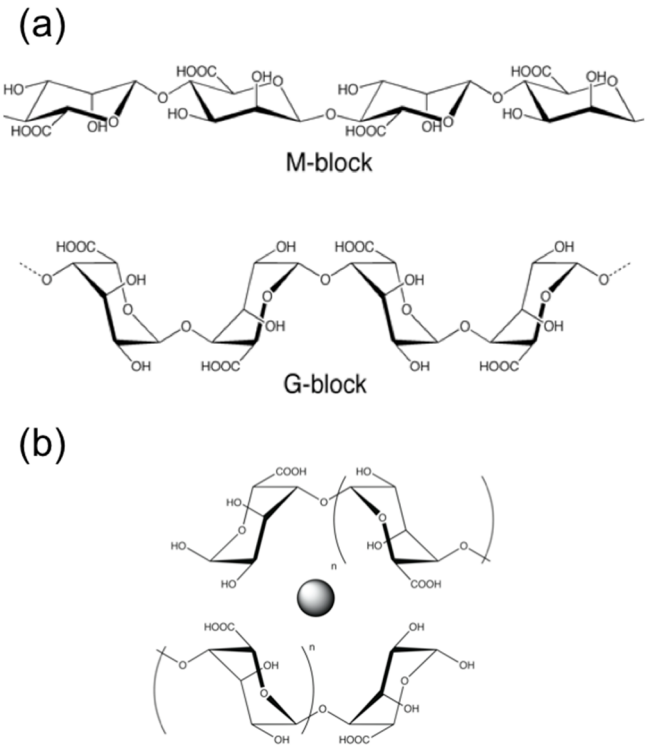

Figure 1 (a) structures of oligoM (oligomannuronic acid) and oligoG (oligoguluronic acid). (b) structure of the 'eggbox' junction zone between two pairs of guluronic acid sequences and a divalent metal cation such as calcium.

We set out to establish the minimum length of oligoG required to form a stable eggbox junction zone and to characterise the onset of eggbox formation using single molecule force spectroscopy measurements conducted by atomic force microscopy (AFM). AFM has previously been used to investigate the binding of the epimerise AlgE4 to its alginate substrate, to study the effect of oligoGs on reducing the interactions between alginate and mucins as well as in an attempt to characterise the relative proportions of M and G in alginates based upon the presence or absence of the chair-boat transition (Sletmoen, Maurstad, Nordgård, Draget, & Stokke 2012; Sletmoen, Skjåk-Bræk, & Stokke, 2004; Williams, Marshall, Haverkamp, & Draget, 2008). The availability of such a single molecule measurement method, in conjunction with a series of nearly monodisperse

oligoguluronic acids, allows us to explicitly measure for the first time the strength of interaction between oligosaccharide pairs in an eggbox junction.

2. Method

2.1.1. Preparation of purified oligoGs. OligoGs were fractionated from partially hydrolysed polyG by size exclusion chromatography and freeze dried as previously described (Ballance et al., 2005). Size was assessed with HPAEC-PAD and compositional purity F(G) and degree of polymerisation (DP(n)) were calculated according to both of the methods described in a previous work (Grasdalen, Larsen, and Smidsrød, 1979) from ^{1}H-NMR spectra recorded on a Bruker Avance 400 MHz spectrometer (Campa et al., 2004): the results are presented in **Table 1**. It is likely that the values of DP(n) for G10 calculated from the NMR spectra are underestimated since, because of the limited amount of material available, the reducing end signals are difficult to determine precisely. The HPAEC-PAD chromatogram for G10 shows very little material at G<10. HPAEC-PAD chromatograms and NMR spectra of the oligoGs are presented in **Supplementary Material**.

Principal OligoG peak (HPAEC-PAD)	F(G)	DP(n)	No. eggbox binding sites
6	0.94	6.05	2
7	0.97	7.02	3
10	0.95	8.3	4
12	0.97	12.83	6
16-18	0.95	20.2	8-10

Table 2 Purities (F(G)) and lengths (DP(n)) of OligoGs used in this study, as determined by NMR and HPAEC-PAD.

2.1.2. Covalent end-linking of oligoG to AFM probes and mica surfaces. Figure 2a depicts the strategy used to conjugate the oligoGs to the AFM probe and mica substrate. (i) OligoGs were functionalised with Boc-NH-PEG-NH_2 (an amine-terminated poly(ethylene glycol) (PEG) with a *tert*-butoxycarbonyl (Boc) protecting group) using a reductive amination method Gray, 1978) previously demonstrated for covalently linking polysaccharides to AFM probes and substrates (Takemasa, Sletmoen, & Stokke, 2009). (ii) The deprotected amine group on the oligoG-PEG conjugate was (iii) coupled to a N-hydroxysuccinimide-PEG-maleimide (NHS-PEG-Mal) and this conjugate was (iv) coupled to either an AFM probe or a mica surface, both functionalised with thiol groups following a method previously used to functionalise silica beads (Gunning, Bongaerts, & Morris, 2009). **Figure 2b** shows the expected disposition of the conjugates during the AFM dynamic force spectroscopy experiments. The two PEGs have expected lengths of 20 nm and 5 nm, and the oligoGs range in length from 3 to 10 nm, so during stretching of a Ca^{2+}-mediated crosslinking bond the maximum length reached before rupture should be approximately 53-60 nm. In the illustration presented, the oligoGs address each other in an antiparallel configuration although a parallel configuration is also possible.

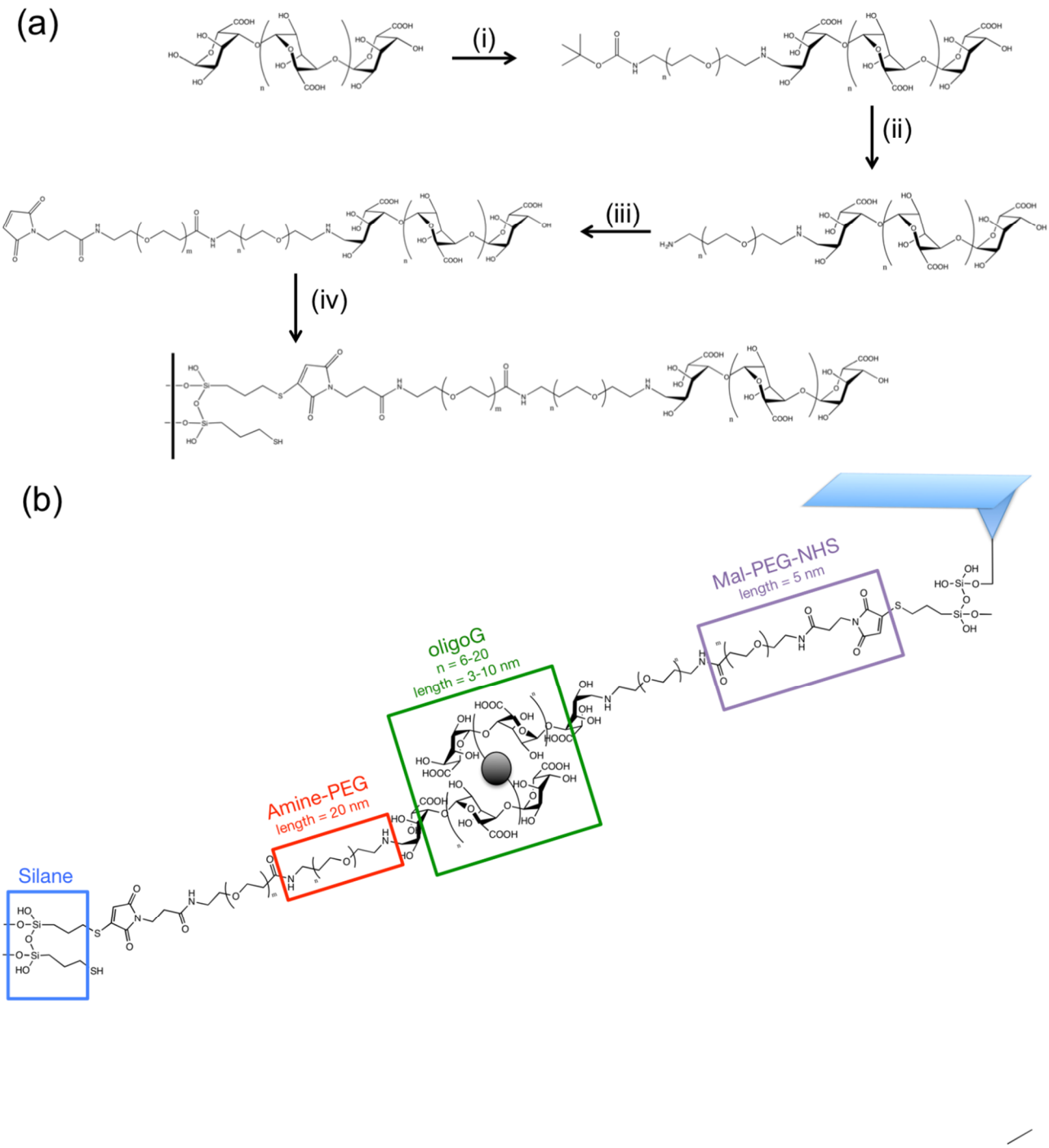

Figure 2 (a) Functionalisation strategy for coupling oligoGs to AFM probe and mica substrate. Steps (i) to (iv) are described in the text. (b) OligoG-PEG constructs on AFM probe and mica substrate during a Ca^{2+}-mediated crosslinking event.

Experimental details of the four steps are as follows: (i) 0.5 mL of 5 M Na BH_3CN (5.0 M solution of sodium cyanoborohydride in aqueous ~1 M sodium hydroxide, Sigma-Aldrich), 250 µL of 0.5 mM aqueous solution of Boc-NH-PEG_{3000}-NH_2 (Iris Biotec, Germany, polydispersity index = 1.03),

1.5 mL of acetate buffer (pH = 5.5), 0.1 mL of 0.5 mM oligoG and 1.5 mL of milliQ water were mixed and incubated for 48 h. (ii) The Boc group on the PEG was deprotected with 50% TFA on ice for 2 h. (iii) 1 μL of NHS-PEG-Mal (SM(PEG)12, ThermoFisher Scientific, 250 mM in DMSO) was added to the oligoG-PEG-NH_2 in PBS, pH 7.2 and incubated for 30 minutes. This product was stored at -20 °C. (iv) AFM probes (MLCT microlevers, Bruker, nominal tip radius = 20 nm, nominal spring constant = 10 pN/nm) or mica surfaces were incubated with a 2% solution in acetone of 3-mercaptopropyltrimethoxysilane (MTS) for 20 minutes, then washed with milliQ water. 100 μL of the oligoG-PEG conjugate produced by step (iii) was incubated with the AFM probes or mica surfaces for 2 h at room temperature or overnight at 4 °C. Functionalised surfaces and probes were used immediately.

2.2.1. AFM force spectroscopy experiments. Force spectroscopy experiments were carried out using a JPK Nanowizard III (JPK, Berlin, Germany) in buffered aqueous solution. Spring constants (calibrated using the method built in to the JPK AFM and based on the method devised by Hutter & Bechhoefer, 1993) ranged from 13.3 to 40.4 pN/nm. Experiments were conducted in 20 mM MOPS (3-morpholinopropane-1-sulfonic acid), with the addition of 2 mM $CaCl_2$ and/or 20 mM EDTA as described. Force curves were collected in arrays of 32 × 32 data points over areas of 2 × 2 microns at a relative setpoint of 0.2 nN. The z-length was 200 nm, dwell time at the surface varied from 0 to 500 ms as described in the text and the approach and retract speeds were set at 500 $nm.s^{-1}$. Thus, total time for an approach and retract cycle with 0 ms dwell was 800 ms and the time the probe and substrate were within 2 PEG-oligoG hydrodynamic radii (approximately 5-12 nm, assuming the PEG is a random coil and the oligoG is a rod with the length of each G monomer set at 0.435 nm (Atkins, Nieduszynski, Mackie, Parker, & Smolko, 1973) of each other (representing the maximum time available for bonds to be formed in a single approach) was 10-25 ms.

2.2.2. Analysis of Dynamic Force Spectra (DFS). Force curves were exported and analysed using JPK's data processing software (JPK instruments, DE, ver. 4.2.23). The observed polymer stretching followed by unbinding events (occurring at a frequency of <10% in all cases) were fitted with an extended freely-jointed chain model and those events with fitted contour lengths in the interval 20 - 80 nm were selected for analysis using the Friddle-Noy-De Yoreo model (Friddle, Noy, & De Yoreo, 2012; Noy & Friddle, 2013) for the forced rupture of bonds using OriginPro™ (OriginLab, ver. 8.0724) as described in the **Supplementary Material**. DFS (plots of □*f*□ vs. ln(r)) were then constructed and the values for the parameters f_{eq} (equilibrium rupture force), x_t (distance to transition state), k_{off} (kinetic off-rate) and ΔG_{bu} (free energy of unbinding) were extracted from fits of the Friddle-Noy-De Yoreo model to the DFS for each oligoG. Values for the work of separation, W_{sep}, were estimated using the JPK data processing software. The Friddle-Noy-De Yoreo model has recently been applied to the crosslinking of DNA by bisintercalators (Rackham, Howell, Round, & Searcey, 2013) while analysis of W_{sep} from force spectra has previously been used to characterise the interaction between alginate oligomers and mucins (Sletmoen et al., 2012).

3. Results and Discussion

3.1. AFM of interactions between oligoGs. OligoGs with lengths from 6 to 20 monomers were coupled to short PEG spacers and attached to both an AFM probe and a mica surface and force curves were collected in the absence and presence of 2mM $CaCl_2$ before addition of 20 mM EDTA. Because the stoichiometry of the GG-Ca^{2+}-GG eggbox junction zone complex is 2:1:2 (see **Figure 1**), the series of oligoGs used can form complexes between pairs of oligoGs by complexation with approximately 2, 3, 4, 6 and up to 10 Ca^{2+} ions (**Table 1**). The PEG-coupling reaction requires the opening of the reducing end sugar, potentially disrupting the Ca^{2+} binding site so that in some cases the number of available Ca^{2+} binding sites will be reduced. Hereafter we classify the oligoGs used

in the experiments in terms of the maximum number of eggbox binding sites that can accommodate Ca^{2+} ions that they possess.

Figure 3 shows a representative selection of force curves obtained from these experiments. In nearly all the observed cases the rupture point in the force curve is sharp but in rare cases there appears to be a short plateau in the force immediately prior to final rupture (**Figure 3a, bottom curve**). When the two PEG-oligoG conjugates approach each other in the presence of a divalent cation they may form an eggbox-like crosslink in either of two configurations (**Figure 3b**): a parallel configuration in which the non-reducing ends of the oligoGs align with each other and an antiparallel configuration in which the non-reducing ends are at opposite ends of the cross linked region. Rupturing the crosslinks in each configuration would be expected to give different results, in that in the antiparallel configuration the direction of pulling at opposite ends of the crosslink will produce an instantaneous failure of the crosslink resulting in a sharp rupture at a high instantaneous force while in the parallel case the crosslink will 'unzip' one monomer at a time at a lower force along the length of the crosslink as the pulling direction will be from the two reducing ends. The situation resembles the forced separation of the two strands of duplex DNA (Clausen-Schaumann, Rief, Tolksdorf, & Gaub, 2000; Essevaz-Roulet, Bockelmann, & Heslot, 1997; Rief, Clausen-Schaumann, & Gaub, 1999) and the coexistence of rupture modes has been observed in the separation of oppositely-charged polyelectrolytes (Spruijt, van den Berg, Cohen Stuart, & van der Gucht, 2012). Because most of the rupture events we record are sharp we find that the typical crosslink observed in these studies is an antiparallel crosslink. This observation is consistent with the proposition that we are rupturing eggbox junction zones. Alternative crosslinking mechanisms, such as the perpendicular crosslink revealed by molecular dynamics simulations (Stewart, Grey, Vasiljevic, & Orbell, 2014), as well as the 'tilted eggbox' proposed by Borgogna et al (Borgogna, Skjåk-Bræk, Paoletti, & Donati, 2013), would also be expected to manifest in a force spectrum as sharp rupture events and so are also compatible with the observed data.

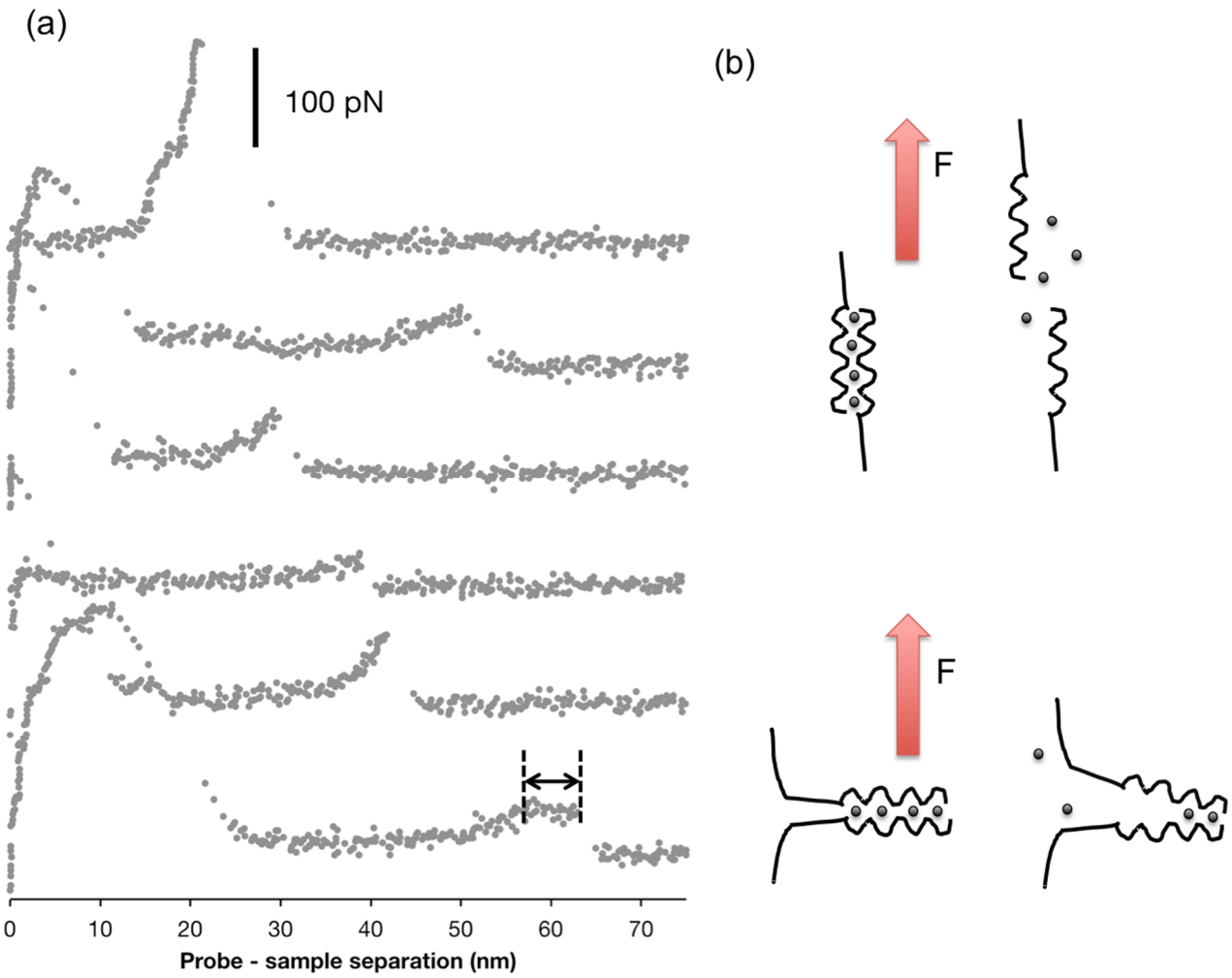

Figure 3 (a) representative force curves obtained from the separation of oligoG pairs in the presence of Ca^{2+}. The bottom curve shows an example of a plateau (approx. 6 nm long) in the recorded force prior to rupture, indicative of a parallel configuration between the oligoGs. (b) sketches of the antiparallel (top) and parallel configurations of pairs of oligoGs in the presence of Ca^{2+} during forced separation. The arrow indicates the direction of the applied force F and Ca^{2+} ions are represented by spheres.

3.2. Distinguishing single and multiple bond rupture events. It is not possible to control the number of bonds formed and broken during a rupture event, beyond adjusting the concentration of participating polymers at the probe and substrate surfaces. It should also be noted that Ca^{2+}-mediated crosslinks may form 'bundles' of 3 or more G-blocks in parallel, which would result in

several polymers being stretched during the rupture of a single 'bundle'. To distinguish the ruptures of single pairs of oligoGs from both these alternatives, we have applied a selection criterion based upon the fitted Kuhn length (Guo, Li, Lad, Desai, & Akhremitchev, 2010), as described in the **Supplementary Material**. We find that the proportion of single bond rupture events identified using this method decreases in the order 2 > 3 > 10 > 6 > 4-site oligoG, with the proportion ranging from 35% down to 17%. Dynamic force spectra for all the data used are presented in **Supplementary Material**.

3.3. Single bond dynamic force spectra. Using this selection criterion, we analyse the W_{sep} distributions and dynamic force spectra for the single bond rupture events in the oligoG series (**Figure 4**). The single bond W_{sep} distribution reveals a discontinuity between the 2-, 3- and 10-site oligoGs on the one hand, with mean W_{sep} values of approximately 0.6 nN.nm, and the 4-site oligoG on the other, with a mean W_{sep} value of 2.4 nN.nm. The 6-site oligoG distribution sits intermediate between these two sets of distributions. Of particular interest here is the distribution for the longest oligoG, the 10-site oligoG, as it encompasses lower values of W_{sep} than the 4- and 6-site oligoGs, indicating the loss of a strong interaction between the oligoG pairs. Very few interactions were observed in the absence of $CaCl_2$ or in the presence of EDTA and those that did occur ruptured over a wide range of W_{sep}, suggesting that they represent non-specific adhesion events (see **Supplementary Material**). The discontinuity in the magnitudes of W_{sep} between junction zones made by 3-site oligoGs and those made by 4-site oligoGs suggested that when 8 guluronic acids were present in each of the paired sequences a much stronger bond was formed. Likewise, the dynamic force spectrum for single unbinding events emphasises the difference between the 4- and 6-site oligoGs on the one hand and the 2-, 3- and 10-site oligoGs on the other. **Table 2** lists the values of the parameters that produce the best fit to the data. These values show differences between the oligoGs: the values of k_{off} for the 4- and 6-site oligoGs are significantly lower than the other oligoGs in the single bond rupture data (6 and 21 s^{-1} respectively vs. 31-53 s^{-1}), suggesting that in these cases there are longer-lived bonds formed. The values for f_{eq} for the 4- and 6-site

oligoGs are approximately double those for the 2-, 3- and 10-site oligoGs while in all cases the value of x_t is close to 0.1 nm, indicating a single bond interaction (Friddle et al., 2012). This latter measure supports our use of the Kuhn length as a selection parameter for single bond ruptures. A similar analysis of the multiple bond interactions, before Kuhn length selection, was also carried out with broadly similar results and is presented as **Supplementary Material**.

Applying the Friddle-Noy-De Yoreo model we can calculate values for the minimum free energy difference between the bound and unbound states (ΔG_{bu}) from the values of f_{eq} obtained at the low loading rate limit of the dynamic force spectrum (**Equation S2.3**). We find values of ΔG_{bu} ranging from 11 to 17 kJ/mol (equivalent to approximately the strength of a hydrogen bond (Hakem, Boussaid, & Benchouk-Taleb, 2007; Suresh & Naik, 2000)) for the 2-, 3- and 10-site oligoGs, indicating a weak interaction, and increasing to 42-144 kJ/mol (equivalent to approximately 3-10 times the strength of a hydrogen bond) for the 4- and 6-site oligoGs. The free energy values for the 4- and 6-site oligoGs indicate the onset of a stronger interaction. Previous calculations (Braccini & Perez, 2001; Fang et al, 2007; Plazinski, 2011) have given values for the energy of an eggbox junction ranging from -25 to -60 kJ/mol per Ca2+ ion, or -107 kcal/mol (-448 kJ/mol) for the dimerisation of guluronate dodecamers. Assuming a linear relationship between junction length and energy these values correspond to approximately -100-300 kJ/mol for an octamer possessing 4 Ca^{2+} binding sites. We obtain a maximum value of ΔG_{bu} for the 4-site oligoG of 144 kJ/mol (**Table 2**) that falls within the lower end of this range, which is in good agreement given that this measurement is likely to include a proportion of weak interactions and is based on the shortest-lived bonds.

Caution must be exerted in comparing the values of W_{sep} and ΔG_{bu} obtained from these analyses as they reflect different situations. Even when we consider only the single bond rupture events, the calculated values of W_{sep} include both the near-equilibrium and far-from-equilibrium situations whereas ΔG_{bu} represents only the former case. Therefore it is expected that the W_{sep} values are much higher than the ΔG_{bu}, and this proves to be the case.

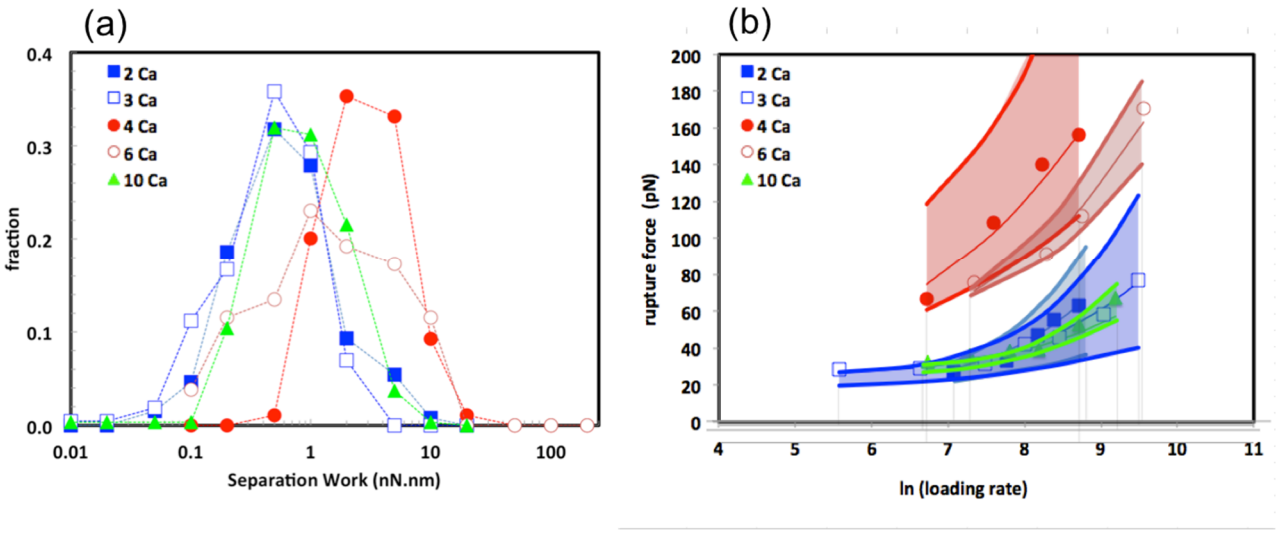

Figure 4 (a) Histograms of work of separation distributions for single bond rupture events in the oligoG series. Note the logarithmic scale of the x-axis. (b) Dynamic force spectra for the same oligoG series. The shaded areas reflect one standard deviation above and below the curves fitted to the Friddle-Noy-De Yoreo model.

OligoG (binding sites)	**2**	**3**	**4**	**6**	**10**
W_{sep}(nN.nm)	0.46 (0.39)	0.60 (0.48)	2.41 (2.16)	1.37 (1.57)	0.67 (0.59)
x_t(nm)	0.15 (0.10)	0.10 (0.10)	0.08 (0.11)	0.07 (0.03)	0.10 (0.01)
k_{off}(s^{-1})	31.9 (23.3)	53.4 (31.8)	6.3 (3.4)	20.9 (6.7)	45.8 (8.1)
f_{eq}(pN)	26.3 (3.3)	24.8 (4.7)	73.0 (6.9)	59.0 (6.0)	25.7 (2.9)
ΔG_{bu}(kJ.mol^{-1})	17.4 (4.4)	11.1 (4.2)	143.9 (27.0)	41.7 (7.0)	13.9 (6.8)

Table 2 Values of W_{sep} and of parameters fitted to Friddle-Noy-de Yoreo model for single bonds for oligo-G series with 2-10 binding sites. Values in parentheses are SD.

3.4. Minimum G-block sequence required for eggbox crosslinking. The data presented here constitute the first single molecule study of the onset of eggbox crosslinking in alginate. In the absence of Ca^{2+} and after addition of EDTA to the samples we observe very few interactions, so we attribute both of the interactions we observe, at high and low W_{sep}, to Ca^{2+}-dependent interactions between oligoGs. Analysis of the distribution of W_{sep} and of the dynamic force spectra for single bond rupture events in oligoGs ranging from 6 to 20 guluronic acids in the presence of Ca^{2+} reveals discontinuities in the distributions of W_{sep}, f_{eq} and k_{off} between oligoGs capable of binding 3 and 4 Ca^{2+} ions. The interaction observed then becomes weaker for longer oligoGs. The increase in interaction strength may be accounted for by proposing the existence of two different interactions between oligoG pairs in the presence of Ca^{2+}: a weak interaction (equivalent in strength to a hydrogen bond) for oligoGs up to 6/7 monomers long; and a stronger interaction that forms only when the oligoG contains 8 monomers (long enough to incorporate 4 Ca^{2+}ions in the junction zone).

This result reflects our current understanding that the minimum length of a stable junction zone is 8 guluronic acids, capable of complexing 4 Ca^{2+}ions (Stokke et al., 1993) and so we identify the strong interaction observed for the 4-site oligoG as the eggbox junction zone. Candidates for the identity of the weaker interaction may be the 'tilted eggbox', formed at low ratios of Ca^{2+} to G in alginates (Borgogna, Skjåk-Bræk, Paoletti, & Donati, 2013) or the perpendicular junction involving 3 Ca^{2+}ions identified by Stewart et al (Stewart, Gray, Vasiljevic, & Orbell, 2014) from molecular dynamics simulations.

3.5. Observing the onset of eggbox junction zone crosslinking. The second trend, a decrease in interaction strength that we observe with larger oligoGs, is counterintuitive: the strength of the interaction between the pairs of the junction zone as reflected by W_{sep} would be expected to increase with length of junction zone. NMR analysis confirmed the sequence lengths and purities of the oligoGs used (**Table 1**), but a consideration of the nature of the DFS experiment suggests a possible reason for the decrease in W_{sep} for the longer junction zones: the probe and surface spend only a short time in sufficiently close proximity to each other for bonds to form (in the data discussed here, the maximum time is approximately 20 ms, see **Methods** section). Thus it may be speculated that on this timescale longer eggbox junction zones do not have enough time to form, and the weaker interaction seen in the shortest oligoGs forms instead. However, the longer oligoGs still contain sequences capable of forming the eggbox junction zone seen in the 4-site oligoG, so this interpretation only explains why the 10-site oligoG does not form a stronger bond than the 4-site oligoG. For the strong interactions observed in the 4-site oligoGs to be absent in the longer oligoGs requires an additional constraint on the formation of those strong interactions to be relevant in those longer oligoGs. In order to establish whether the eggbox crosslinks are kinetically disfavoured or entirely prevented from forming in the longest oligoGs, and to gain some insight into what this additional constraint might be, we extended the dwell time of the AFM probe at the substrate surface.

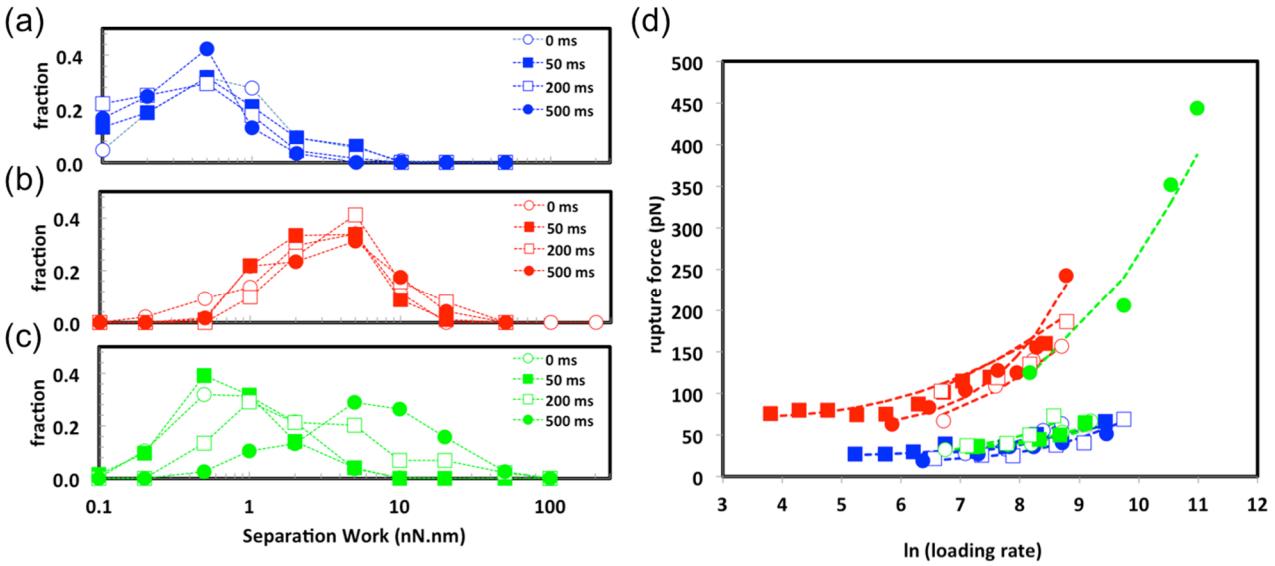

Figure 5 (a-c) Histograms of work of separation distributions for single bond rupture events in the oligoG series with capacities of (a) 2, (b) 4 and (c) 10 Ca^{2+}ions with increased surface dwell times of 50, 200 and 500 ms. (d) Dynamic force spectra for single bond rupture events in the same oligoG series, overlaid to highlight the shift from weak to strong interaction.

The hypothesis that junction zones longer than 8 monomers take longer than 20 ms to form was tested for the 2-, 4- and 10-site oligoGs by increasing the dwell time of the AFM probe at the surface to from 0 to 50, 200 and 500 ms (giving total times that the probe and sample are within 20nm of each other of 20, 70, 220 and 520 ms). **Figure 5** shows how the work distributions for single bond rupture events (selected using the same Kuhn length criterion as described above) changed as the dwell time was increased. For the 2- and 4-site oligoGs the work distributions showed little to no change when the interaction time at the sample surface was increased from 20 to 520 ms (for 2-site oligoGs mean W_{sep} ranges from 0.32 to 0.50 $nN.nm^{-1}$ and for 4-site oligoGs it varies from 2.20 to 3.75 $nN.nm^{-1}$), suggesting that for these oligoGs 20ms is sufficient time for the maximum possible interaction to form, and in the case of the 4-site oligoG that this is enough time for the egg-box junction zone to displace the weaker Ca^{2+}-dependent interaction. However, for the longest oligoG, consisting of up to 10 junction zone units, the work distribution changed significantly, shifting from being identical to the 2-site oligoG at 20 and 70 ms (mean W_{sep} = 0.44

$nN.nm^{-1}$) to higher values of W_{sep} at 220 and 520 ms (1.03 to 6.10 $nN.nm^{-1}$). From this we conclude that the largest junction zone that can form between oligoGs of 20 residues takes longer than 220 ms to displace the initial, weak bond(s) that is (are) formed, and may not yet have reached equilibrium after 520 ms. When interaction times exceed 220 ms, the expected dependence of interaction strength on oligo length is restored. **Table 3** presents the values of the kinetic and thermodynamic parameters fitted to the Friddle-Noy-De Yoreo model. In the 4-site oligoG at all dwell times and in the 10-site oligoG at 500 ms dwell time, the fits show: values for x_t close to 0.1 nm for all datasets, supporting the Kuhn length selection method for isolating single bond ruptures; lower values for k_{off}, signalling longer-lived bonds; and higher f_{eq} values. These parameters are in agreement with the W_{sep} distributions in identifying the 4-site oligoG interactions at all dwell times and the 10-site oligoG interaction at 500 ms dwell time as eggbox-like crosslinks.

OligoG binding sites	**2**	**2**	**2**	**4**	**4**	**4**	**10**	**10**	**10**
Dwell time (ms)	50	200	500	50	200	500	50	200	500
W_{sep}(nN.nm)	0.50 (0.55)	0.34 (0.36)	0.32 (0.29)	2.38 (2.12)	3.75 (3.49)	3.22 (3.14)	0.44 (0.52)	1.03 (1.44)	6.10 (5.70)
x_t(nm)	0.15 (0.05)	0.09 (0.05)	0.14 (0.05)	0.10 (0.03)	0.09 (0.04)	0.08 (0.04)	0.08 (0.02)	0.06 (0.02)	0.06 (0.02)
$k_{off}(s^{-1})$	24.2 (18.4)	77.9 (33.9)	46.4 (28.8)	8.7 (4.2)	12.2 (5.6)	10.3 (4.3)	74.2 (29.6)	49.3 (20.1)	12.9 (4.8)
f_{eq}(pN)	24.0 (2.9)	16.0 (2.1)	19.0 (2.8)	58.0 (6.1)	55.0 (6.9)	64.0 (6.6)	30.0 (3.4)	26.0 (6.3)	67.0 (7.1)
ΔG_{bu} ($kJ.mol^{-1}$)	14.7 (3.6)	6.6 (1.8)	9.2 (2.9)	90.9 (19.1)	81.7 (17.5)	110.6 (22.8)	14.8 (3.4)	11.1 (5.4)	73.9 (15.7)

Table 3 Values of W_{sep} and of parameters fitted to Friddle-Noy-De Yoreo model for single bond rupture events for 2-, 4- and 10-site oligoGs at 50, 200 and 500 ms dwell times. Values in parentheses are SD.

We can compare this experimental approach and these findings to previous studies of the onset of alginate gelation. Both Borgogna et al., (2013) and Fang et al., (2007) studied the onset of alginate gelation by limiting the amount of Ca^{2+} present, using ratios of Ca^{2+}:G (R^{Ca2+}) between 0 and 0.4. In

both cases eggbox crosslinking started to occur at Ca^{2+}:G ratios of between 0.13 and 0.25, corresponding to Ca^{2+} concentrations in the range 0.15 - 0.6 mM. In the present work we used 2 mM Ca^{2+} in all experiments and instead varied the time that opposing oligoGs were in close enough proximity to interact. This approach is analogous to one where the local concentration of oligoGs is varied transiently under conditions of constant [Ca^{2+}]. Borgogna et al., (2013) found a negative dependence of the minimum R^{Ca2+} at which eggbox crosslinking was observed on the concentration of G, following the relationship $R^{Ca2+}_{min} \propto 1/[G]^{1/2}$. This translates into a positive dependence of the actual concentration of Ca^{2+} present on [G], so that $[Ca^{2+}]_{min} \propto [G]^{1/2}$. Thus, as the local concentration of G-blocks increases (and as their length increases), the minimum concentration of Ca^{2+} required to induce eggbox crosslinking also increases. Thus we need to estimate this minimum concentration for the effective concentration of G in these experiments in order to establish whether we are working in conditions of limiting or excess Ca^{2+}. Estimating the effective [G] in the interaction volume between the AFM probe and surface during the time that both are within two hydrodynamic radii of each other depends on variables that can only be estimated imprecisely: from our fits to the DFS we can estimate the average number of bonds made between the probe and sample in one approach-retract cycle, and we can estimate the size of the interaction volume from the radius of the AFM probe's tip (20 nm) and the hydrodynamic radii of the PEG-oligoGs (10 nm); if we then make the assumption that all the oligoGs within the interaction volume during an approach-retract cycle take part in crosslinking interactions we can estimate an effective [G] of approximately 3 mM (see **Supplementary Material**). This is likely to be a minimum value because it assumes that all the oligoGs within the interaction volume form bonds with oligoGs on the opposing surface during an approach-retract cycle, an assumption that we will challenge below. Using this value and the relationship found by Borgogna et al we find that [Ca^{2+}_{min}] = 0.5 mM. Given a bulk [Ca^{2+}] of 2mM, and considering that counterion condensation will be likely to increase the local [Ca^{2+}] in the immediate environment of the oligoGs (Donati, Asaro, & Paoletti, 2009), we

can conclude that the experiments conducted in the present work reflect a condition of excess Ca^{2+} and that eggbox crosslinking is not limited by Ca^{2+} supply as it was in previous studies.

A model for the onset of crosslinking between two semiflexible polyelectrolytes has been proposed (Borukhov, Bruinsma, Gelbart, & Liu, 2001), and may shed some light on the processes underlying the behaviour we have observed in the present work. This model finds that a repulsive barrier exists between two linkers (in this case the Ca^{2+} ions) as the distance between crosslinks along the polyelectrolyte chains (in this case the oligoGs) decreases. This repulsion arises from electrostatic repulsions between the linkers themselves and between the opposing polyelectrolyte chains, giving rise to the observation that single crosslinks will be most favoured by a crossing angle between the two polyelectrolyte chains of 90° so that electrostatic repulsion between the polyelectrolytes is minimised. In the dense crosslink regime, reflecting the eggbox crosslinks, the polyelectrolytes are aligned (angle = 0°) and so another repulsion barrier arises from the chain linker stiffness opposing this rearrangement between the chains until the distance between linkers becomes small and the chains are aligned, where chain stiffness starts to favour the extension of the region of dense crosslinks. Thus this model predicts that once an eggbox crosslink is established, the stiffness of the polyelectrolyte chains should drive their continued alignment and allow the junction zone to extend to the maximum extent possible (i.e. the full length of the oligoG), which contradicts the evidence we have for the longest oligoGs at short interaction times.

Reconciliation between this model and our data is possible when we consider the distribution of oligoGs at the probe and substrate surfaces. We found that the average number of interactions between probe and substrate per unbinding event was approximately 20 (based upon the value of x_t presented in **Table S1**), occurring in an area of approximately 9×10^{-16} m^2 (see **Supplementary Material**) but that unbinding events were only recorded in less than 10% of approach-retract cycles, suggesting that the coverage of oligoGs on the substrate and probe was anisotropic and that instead of a uniform, dilute coverage of oligoGs at the surfaces there are regions of dense coverage where the oligoGs are clustered close together. In this situation, Ca^{2+}- mediated crosslinks may be

occurring between closely neighbouring oligoGs on the AFM probe or on the substrate, and when these interactions occur between oligoGs on the same surface they are not detected by the force spectroscopy experiment. The distance between oligoGs at which these unobserved interactions may occur increases with the length of the oligoGs, so this effect will be more relevant for the longest oligoGs. We can then envisage a situation (illustrated in **Figure 6**) in which a single oligoG chain takes part in interactions with two oligoGs, one on the same surface and one on the opposing surface. With the shortest oligoGs this effect will be absent since the chains are likely not long enough to participate in two independent interactions, while for the 4-site oligoG it is only possible for two weak interactions to form, and one is likely to displace the other and proceed to eggbox formation: when the dominant interaction is the intersurface one, then a strong interaction will be seen in the force spectroscopy data and when it is the intrasurface interaction that dominates then no interaction will be observed. It is only in the longest oligoG, with up to 20 monomers and 10 Ca^{2+} binding sites, where the possibility arises that both an incipient eggbox junction and a single linker interaction may occur simultaneously. When the time available for interactions between surfaces is short, the link formed between the rapidly separated oligoGs on the probe and the substrate will be less likely to proceed to eggbox formation than the link between two oligoGs on the same surface, so in the force spectroscopy experiment we only observe the single linker interaction. As the interaction time increases, the probability that the crosslink between surfaces outcompetes the crosslink on the same surface increases and so we begin to observe long eggbox crosslinks in the 10-site oligoG. The timescale for the resolution of the competition between the two interactions is established by the data we present here as on the order of hundreds of milliseconds. A timescale of tens to hundreds of milliseconds is rather long for a molecular scale event (similar to the typical time for a protein of 100 peptides to fold (Naganathan & Muñoz, 2004)), and we propose that the extended timescale arises from the fact that the oligomers are held under tension as the AFM probe retracts, creating an additional entropic barrier to crosslinking.

This time delay in resolving the interaction between competing bonds can be considered as analogous to the situation that occurs within an alginate gel. Recently dynamic light scattering and direct mechanical analysis of alginate gels (Larobina & Cipelletti, 2013; Secchi, Roversi, Buzzaccaro, Piazza, & Piazza, 2013) has revealed the slow breaking of bonds during the relaxation of maturing alginate gels due to thermal activation and the relieving of internal stresses. These stresses arise when the formation of a crosslink by one section of a polymer constrains another part, leading to the breaking of crosslinks so that the tension may be relieved, as part of a two-stage process that takes up to thousands of seconds to resolve. It can then be seen that the situation we describe for the 10-site oligoG data reflects just this process at the nanoscale, and our estimate of several hundred milliseconds for the resolution of competition between a single crosslink and a 10-site egg box crosslink may correspond to much longer times for the complete relaxation of chains consisting of many thousands of binding sites.

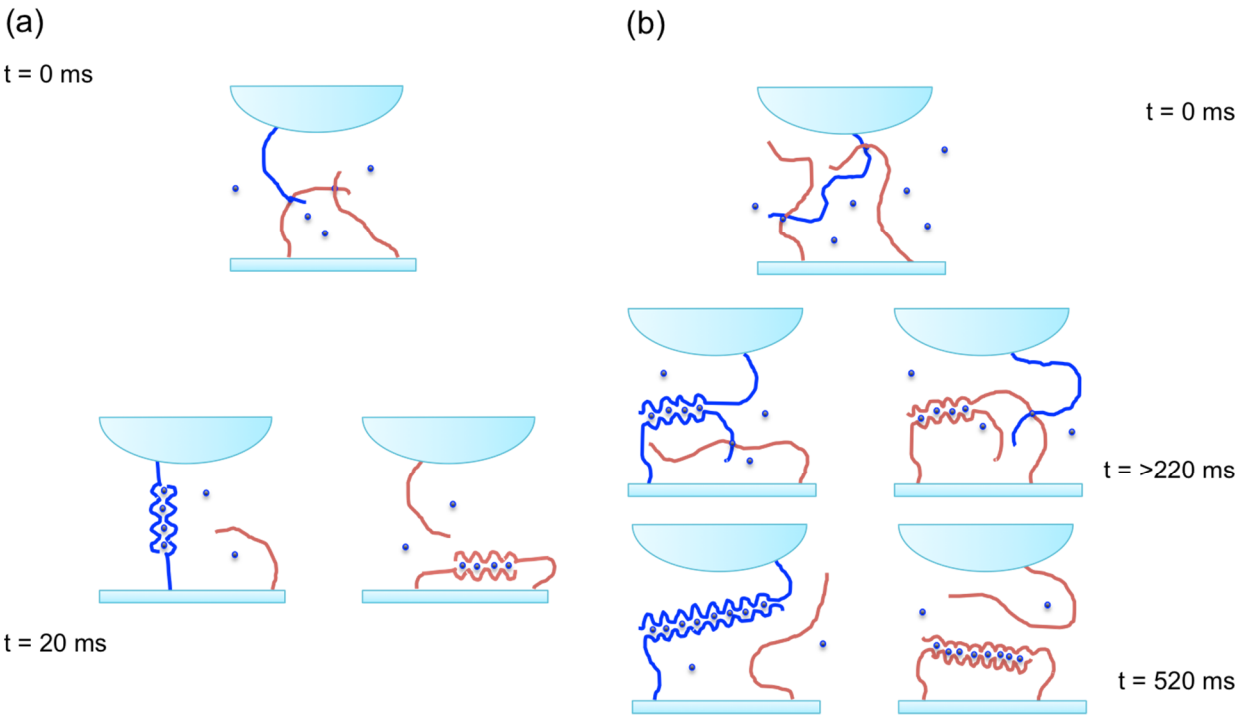

Figure 6 Sketches of the proposed evolution of multiple attachments between oligoG strands attached to AFM probe (top) and substrate (bottom) over time. (a) 4-site oligoG, t = 0 and 20 ms; (b) 8-site oligoG, t = 0, 220 and 520 ms. Dark blue interactions are detected by the force spectroscopy experiment, pale red ones are not.

4. Conclusion

The aims of this work were to establish, at the single molecule level, the minimum sequence of pairs of guluronic acids necessary to induce a strong junction zone in the presence of Ca^{2+}, and thence to characterise the onset of this minimum junction zone and follow its evolution to longer junctions. We have shown experimentally for the first time that pairs of at least 8 guluronic acids are required to form a strong, stable Ca^{2+}-mediated junction zone. The apparent reduction in strength of crosslinks formed by longer oligoGs at short interaction times is revealed to be a consequence of the constraint on propagation of the crosslinks that is caused by the 'pinning' effect of parallel, weaker, crosslinks formed at other points along the polymer. We estimate a timeframe of several hundred milliseconds for the resolution of this stress in oligoG blocks up to 20 units in length. In the context of alginate gelation and the relaxation processes that contribute to the rheology of alginate gels this data provides molecular-level insight into the processes that govern the release of internal stresses, identified recently (Larobina & Cipelletti, 2013; Siviello, Greco, & Larobina, 2015) as a critical mechanism in alginate gel rheology.

Acknowledgements

The authors would like to acknowledge funding from Biotechnology and Biological Sciences Research Council (UK) grant H019294 (KB and AR); Norwegian Research Council grant MARPOL 10 399 200 (OA and GS-B) and Science Without Borders (MN).

References

Atkins, E. D.; Nieduszynski, I. A.; Mackie, W.; Parker, K. D.; Smolko, E. E. Structural components of alginic acid. II. The crystalline structure of poly-alpha-L-guluronic acid. Results of x-ray diffraction and polarized infrared studies. *Biopolymers* **1973**, *12*, 1879–1887.

Ballance, S.; Holtan, S.; Aarstad, O. A.; Sikorski, P.; Skjåk-Braek, G.; Christensen, B. E. Application of high-performance anion-exchange chromatography with pulsed amperometric detection and statistical analysis to study oligosaccharide distributions--a complementary method to investigate the structure and some properties of alginates. *Journal of Chromatography A* **2005**, *1093*, 59–68.

Borgogna, M.; Skjåk-Braek, G.; Paoletti, S.; Donati, I. On the initial binding of alginate by calcium ions. The tilted egg-box hypothesis. *Journal Of Physical Chemistry B* **2013**, *117*, 7277–7282.

Borukhov, I.; Bruinsma, R. F.; Gelbart, W. M.; Liu, A. J. Elastically driven linker aggregation between two semiflexible polyelectrolytes. *Physical Review Letters* **2001**, *86*, 2182–2185.

Braccini, I.; Perez, S. Molecular basis of Ca(2+)-induced gelation in alginates and pectins: the egg-box model revisited. *Biomacromolecules* **2001**, *2*, 1089–1096.

Campa, C.; Holtan, S.; Nilsen, N.; Bjerkan, T. M.; Stokke, B. T.; Skjåk-Braek, G. Biochemical analysis of the processive mechanism for epimerization of alginate by mannuronan C-5 epimerase AlgE4. *The Biochemical Journal* **2004**, *381*, 155–164.

Campa, C.; Oust, A.; Skjåk-Braek, G.; Paulsen, B. S.; Paoletti, S.; Christensen, B. E.; Ballance, S. Determination of average degree of polymerisation and distribution of oligosaccharides in a partially acid-hydrolysed homopolysaccharide: a comparison of four experimental methods applied to mannuronan. *Journal of Chromatography A* **2004**, *1026*, 271–281.

Clausen-Schaumann, H.; Rief, M.; Tolksdorf, C.; Gaub, H. E. Mechanical stability of single DNA molecules. *Biophysical Journal* **2000**, *78*, 1997–2007.

Donati, I.; Asaro, F.; Paoletti, S. Experimental Evidence of Counterion Affinity in Alginates: The Case of Nongelling Ion Mg2+. *Journal Of Physical Chemistry B* **2009**, *113*, 12877–12886.

Draget, K. I.; Skjåk-Bræk, G.; Smidsrød, O. Alginate based new materials. *International Journal of Biological Macromolecules* **1997**, *21*, 47–55.

Draget, K. I.; Smidsrød, O.; Skjåk-Bræk, G. **2005**. Alginates from Algae. In A. Steinbuchel & S. K. Rhee (Eds.) *Polysaccharides and Polyamides in the Food Industry. Properties, Production and Patents* (pp.1-30). Weinheim: Wiley-VCH.

Draget, K. I.; Taylor, C. Chemical, physical and biological properties of alginates and their biomedical implications. *Food Hydrocolloids* **2011**, *25*, 251–256.

Essevaz-Roulet, B.; Bockelmann, U.; Heslot, F. Mechanical separation of the complementary strands of DNA. *Proceedings Of The National Academy Of Sciences Of The United States Of America* **1997**, *94*, 11935–11940.

Fang, Y.; Al-Assaf, S.; Phillips, G. O.; Nishinari, K.; Funami, T.; Williams, P. A.; Li, L. Multiple Steps and Critical Behaviors of the Binding of Calcium to Alginate. *Journal Of Physical Chemistry B* **2007**, *111*, 2456–2462.

Friddle, R. W.; Noy, A.; De Yoreo, J. J. Interpreting the widespread nonlinear force spectra of intermolecular bonds. *Proceedings of the National Academy of Sciences* **2012**, *109*, 13573–13578.

Gorin, P.; Spencer, J. Exocellular alginic acid from Azotobacter vinelandii. *Canadian Journal of Chemistry* **1966**, *44*, 993-998.

Grant, G. T.; Morris, E. R.; Rees, D. A.; Smith, P.; Thom, D. Biological interactions between polysaccharides and divalent cations: The egg-box model. *FEBS letters* **1973**, *32*, 195-198.

Grasdalen, H.; Larsen, B.; Smidsrød, O. A p.m.r. study of the composition and sequence of uronate residues in alginates. *Carbohydrate Research* **1979**, *68*, 23–31.

Gray, G. Antibodies to carbohydrates: preparation of antigens by coupling carbohydrates to proteins by reductive amination with cyanoborohydride. *Methods in Enzymology* **1978**, *50*, 155-160.

Gunning, A. P.; Bongaerts, R. J. M.; Morris, V. J. Recognition of galactan components of pectin by galectin-3. *The FASEB Journal* **2009**, *23*, 415–424.

Guo, S.; Li, N.; Lad, N.; Desai, S.; Akhremitchev, B. B. Distributions of parameters and features of multiple bond ruptures in force spectroscopy by atomic force microscopy. *The Journal of Physical Chemistry C* **2010**, *114*, 8755–8765.

Hakem, I. F.; Boussaid, A.; Benchouk-Taleb, H. Temperature, pressure, and isotope effects on the structure and properties of liquid water: a lattice approach. *The Journal of Chemical Physics* **2007**, *127*, 224106.

Hartmann, M.; Holm, O. B.; Johansen, G. A. B.; Skjåk-Braek, G.; Stokke, B. T. Mode of action of recombinant Azotobacter vinelandii mannuronan C-5 epimerases AlgE2 and AlgE4. *Biopolymers* **2002**, *63*, 77–88.

Haug, A.; Larsen, B. Biosynthesis of alginate. *Carbohydrate Research* **1971**, *17*, 287–296.

Haug, A.; Larsen, B. Biosynthesis of alginate. II. Polymannuronic acid C-5-epimerase from Azotobacter vinelandii (Lipman). *Carbohydrate Research* **1971**, *17*, 297–308.

Høidal, H. K.; Ertesvåg, H.; Skjåk-Braek, G.; Stokke, B. T.; Valla, S. The recombinant Azotobacter vinelandii mannuronan C-5-epimerase AlgE4 epimerizes alginate by a nonrandom attack mechanism. *The Journal of Biological Chemistry* **1999**, *274*, 12316–12322.

Holtan, S.; Zhang, Q.; Strand, W. I.; Skjåk-Braek, G. Characterization of the hydrolysis mechanism of polyalternating alginate in weak acid and assignment of the resulting MG-oligosaccharides by NMR spectroscopy and ESI-mass spectrometry. *Biomacromolecules* **2006**, *7*, 2108–2121.

Hutter, J. L.; Bechhoefer, J. Calibration of atomic-force microscope tips. *Review Of Scientific Instruments* **1993**, *64*, 1868–1873.

Larobina, D.; Cipelletti, L. Hierarchical cross-linking in physical alginate gels: a rheological and dynamic light scattering investigation. *Soft Matter* **2013**, *9*, 10005–10015.

Larsen, B.; Haug, A. Biosynthesis of alginate: Part III. Tritium incorporation with polymannuronic acid 5-epimerase from Azotobacter vinelandii. *Carbohydrate Research* **1971**, *20*, 225–232.

Linker, A.; Jones, R. S. A new polysaccharide resembling alginic acid isolated from pseudomonads. *The Journal of Biological Chemistry* **1966**, *241*, 3845–3851.

Naganathan, A. N.; Muñoz, V. Scaling of folding times with protein size. *Journal of the Americans Chemical Society* **2004**, *127*, 480-481.

Noy, A.; Friddle, R. W. Practical single molecule force spectroscopy: how to determine fundamental thermodynamic parameters of intermolecular bonds with an atomic force microscope. *Methods (San Diego, Calif)* **2013**, *60*, 142–150.

Plazinski, W; Molecular Basis of Calcium Binding by Polyguluronate Chains. Revising the Egg-Box Model. *Journal of Computational Chemistry* **2011**, *32*, 2988-2995.

Rackham, B. D.; Howell, L. A.; Round, A. N.; Searcey, M. Non-covalent duplex to duplex crosslinking of DNA in solution revealed by single molecule force spectroscopy. *Organic & Biomolecular Chemistry* **2013**, *11*, 8340–8347.

Rief, M.; Clausen-Schaumann, H.; Gaub, H. E. Sequence-dependent mechanics of single DNA molecules. *Nature Structural Biology* **1999**, *6*, 346–349.

Secchi, E.; Roversi, T.; Buzzaccaro, S.; Piazza, L.; Piazza, R. Biopolymer gels with “physical” cross-links: gelation kinetics, aging, heterogeneous dynamics, and macroscopic mechanical properties. *Soft Matter* **2013**, *9*, 3931–3944.

Sikorski, P.; Mo, F.; Skjåk-Braek, G.; Stokke, B. T. Evidence for egg-box-compatible interactions in calcium-alginate gels from fiber X-ray diffraction. *Biomacromolecules* **2007**, *8*, 2098–2103.

Siviello, C.; Greco, F.; Larobina, D. Analysis of linear viscoelastic behaviour of alginate gels: effects of inner relaxation, water diffusion, and syneresis. *Soft Matter* **2015**, *11*, 6045–6054.

Skjåk-Braek, G.; Smidsrod, O.; Larsen, B. Tailoring of alginates by enzymatic modification in vitro. *International Journal of Biological Macromolecules* **1986**, *8*, 330–336.

Sletmoen, M.; Maurstad, G.; Nordgård, C. T.; Draget, K. I.; Stokke, B. T. Oligoguluronate induced competitive displacement of mucin–alginate interactions: relevance for mucolytic function. *Soft Matter* **2012**, *8*, 8413-8421.

Sletmoen, M.; Skjåk-Braek, G.; Stokke, B. T. Single-molecular pair unbinding studies of Mannuronan C-5 epimerase AlgE4 and its polymer substrate. *Biomacromolecules* **2004**, *5*, 1288–1295.

Spruijt, E.; van den Berg, S. A.; Stuart, M. C. Direct measurement of the strength of single ionic bonds between hydrated charges. *ACS Nano* **2012**, *6*, 5297–5303.

Stewart, M. B.; Gray, S. R.; Vasiljevic, T.; Orbell, J. D. Exploring the molecular basis for the metal-mediated assembly of alginate gels. *Carbohydrate Polymers* **2014**, *102*, 246-253.

Stokke, B. T.; Smidsrod, O.; Bruheim, P.; Skjåk-Braek, G. Distribution of uronate residues in alginate chains in relation to alginate gelling properties. *Macromolecules* **1991**, *24*, 4637–4645.

Stokke, B. T.; Smidsrod, O.; Zanetti, F.; Strand, W.; Skjåk-Braek, G. Distribution of uronate residues in alginate chains in relation to alginate gelling properties – 2. Enrichment of beta-D-

mannuronic acid and depletion of alpha-L-guluronic acid in sol fraction. *Carbohydrate Polymers* **1993**, *21*, 39–46.

Suresh, S. J.; Naik, V. M. Hydrogen bond thermodynamic properties of water from dielectric constant data. *The Journal of Chemical Physics* **2000**, *113*, 9727–9732.

Takemasa, M.; Sletmoen, M.; Stokke, B. T. Single Molecular Pair Interactions between Hydrophobically Modified Hydroxyethyl Cellulose and Amylose Determined by Dynamic Force Spectroscopy. *Langmuir* **2009**, *25*, 10174–10182.

Williams, M. A. K.; Marshall, A.; Haverkamp, R. G.; Draget, K. I. Stretching single polysaccharide molecules using AFM: A potential method for the investigation of the intermolecular uronate distribution of alginate? *Food Hydrocolloids* **2008**, *22*, 18–23.